

This is a provisional PDF only. Copyedited and fully formatted version will be made available soon.



ISSN: 0015-5659

e-ISSN: 1644-3284

METTL14 knockdown attenuates neuron injury and improves function recovery after spinal cord injury via regulating FGF21 in a m6A-IGF2BP1 dependent mechanism

Authors: Guozhen Zhang, Bingbing Pu, Fanjun Qin, Qiaojing Lin

DOI: 10.5603/fm.103208

Article type: Original article

Submitted: 2024-10-22

Accepted: 2024-12-06

Published online: 2025-01-09

This article has been peer reviewed and published immediately upon acceptance. It is an open access article, which means that it can be downloaded, printed, and distributed freely, provided the work is properly cited. Articles in "Folia Morphologica" are listed in PubMed.

ORIGINAL ARTICLE

DOI: 10.5603/fm.103208

METTL14 knockdown attenuates neuron injury and improves function recovery after spinal cord injury via regulating FGF21 in a m6A-IGF2BP1 dependent mechanism

Guozhen Zhang, Bingbing Pu, Fanjun Qin, Qiaojing Lin

Fudan University Affiliated Pudong Medical Centre, Shanghai, China

Address for correspondence: Qiaojing Lin, Fudan University Affiliated Pudong Medical Centre, 525 Hongfeng Rd, Pudong, Shanghai, China; e-mail: 13162799150@163.com

ABSTRACT

Background: Fibroblast growth factor 21 (FGF21) and Methyltransferase-like 14 (METTL14) have been identified to be involved in spinal cord injury (SCI). However, whether FGF21 functioned in SCI via METTL14-induced N6-methyladenosine (m6A) modification remains unclear.

Materials and methods: PC12 cells were exposed to lipopolysaccharide (LPS) *in vitro*. qRT-PCR and western blotting analyses were applied to detect the mRNA and protein levels of METTL14, FGF21 and Insulin-like growth factor 2 mRNA-binding protein 1 (IGF2BP1). The CCK-8 assay, EdU assay, flow cytometry and ELISA analysis were used to conduct *in vitro* functional analyses. Cell ferroptosis was assessed by measuring the levels of Fe²⁺, reactive oxygen species, glutathione and related regulators. The N6-methyladenosine (m6A) modification profile was analyzed by methylated RNA immunoprecipitation (MeRIP) assay. The interaction between IGF2BP1 and FGF21 was validated using RIP assay. SCI animal models were constructed for *in vivo* analysis.

Results: Levels of FGF21 were decreased in LPS-induced PC12 cells. Functionally, FGF21 overexpression reversed LPS-induced proliferation inhibition, apoptosis, ferroptosis and inflammation in PC12 cells. Mechanistically, METTL14 induced FGF21 m6A modification in SCI cell models, and m6A-binding protein IGF2BP1 was involved in regulating FGF21

expression by METTL14. METTL14 silencing abolished LPS-induced neuronal apoptosis, inflammation and ferroptosis via regulating FGF21. Moreover, METTL14 silencing improved neuronal injury in SCI rat models by modulating FGF21 expression.

Conclusions: METTL14 knockdown attenuates neuron injury and improves function recovery after SCI via up-regulating FGF21 in an m6A-IGF2BP1 dependent mechanism, suggesting a useful target for SCI recovery.

Keywords: m6A, SCI, ferroptosis, neuroinflammation, FGF21, METTL14, GPX4

INTRODUCTION

Spinal cord injury (SCI) is an insult to the bundle of nerves and nerve fibers, which mediate signals exchange between the brain and body occurs, often caused by trauma and nontraumatic etiologies like degeneration and malignancy [7, 21]. SCI can causes major motor, sensory and autonomic dysfunctions, leading to permanent disability and even mortality [3]. Treatment options for SCI range from conservative, operative, rehabilitative to stem cell therapies requiring long-term investment, however, there are currently no effective treatments to improve neurological state [14, 22]. Accordingly, better understand the pathogenesis of SCI is indispensable for developing effective therapeutic strategy for alleviating the loss of neurological functions.

The pathogenesis resulting in SCIs are classified as either primary or secondary. The initial primary injury causes cell injury, leading to ions imbalance, excitant amino acid release and the production of oxidative species in the injured region [5, 25]. The primary physical lesion subsequently evokes secondary injury accompanied with the injury to healthy adjacent cells, inflammation, neuronal death because of apoptosis and ferroptosis, and eventually function loss [2, 15, 16]. Hence, it is of utmost importance that preventing neuronal inflammation, apoptosis and ferroptosis for improving SCI. Fibroblast growth factor 21 (FGF21) is a stress-inducible hormone involving in modulating energy balance and the homeostasis of glucose and lipid [8]. Currently, FGF21 has attracted great research interest for their therapeutic applications since its pharmacological benefits on correcting metabolic

dysfunction, alleviating insulin resistance and hyperglycaemia, and reducing fat mass associated with obesity and diabetes have been validated in non-human primates or rodents [1, 10]. In SCI, Xu *et al.* showed that FGF21 overexpression suppressed ferroptosis and apoptosis in nerve cells following SCI damage [11, 27]. Decreased FGF21 contributed to metabolic dysfunction after SCI [20]. Forced expression of FGF21 enhanced functional recovery after SCI by suppressing cell autophagy and apoptosis in injured area [29]. Therefore, it is conceivable to foster FGF21 activity as a viable therapeutic target for improving SCI.

Herein, we highlighted the effects and mechanism of FGF21 on SCI-triggered neuroinflammation, neuroapoptosis, ferroptosis, and function dysfunction, which may provide novel insights into pharmacological effects of FGF21 on SCI.

MATERIALS AND METHODS

Cell culture and treatment

PC12 cells were purchased from ATCC (Rockville, MD, USA) and cultured in 1640 medium (Invitrogen, Carlsbad, CA, USA) supplemented with 10% foetal bovine serum (FBS, ATCC), 1% penicillin/streptomycin at 37°C with 5% CO₂.

PC12 cells used for functional analyses were differentiated to obtain neural cell properties by treating cells with 5 µg/L nerve growth factor (NGF) for 72 h. Then cells were collected and exposed to LPS (5 µg/mL, Sigma-Aldrich, MA, USA) for 12 h to establish SCI cell models.

Transient transfection

The overexpression plasmids of FGF21 or IGF2BP1, named FGF21 or IGF2BP1 were constructed using pcDNA3.1 plasmids (GenePharma, Shanghai, China) with scramble plasmids as the control (Vector). Specific small interference RNAs (siRNAs) were designed to target METTL3/4/16, WTAP, ALKBH5, YTH domain family of proteins (YTHDF1/2/3), and insulin like growth factor 2 mRNA binding protein 1/2/3 (IGF2BP1/2/3), or FGF21, named si-METTL3/4/16, si-WTAP, si-ALKBH5, si-IGF2BP1/2/3, si-YTHDF1/2/3 or si-FGF21, and the scramble siRNA was used as the control. The transient transfection was carried out using

Lipofectamine 2000 (Invitrogen) for 48 h.

Western blotting

The isolation of total proteins was performed by incubating cells or tissues with RIPA lysis buffer (Yeasen, Shanghai, China) on ice. The concentration of protein samples was verified using a BCA kit (Beyotime, Beijing, China). Then 10% SDS-PAGE was used to separate protein, and consequent proteins were shifted onto PVDF membranes. Following 1 h blockage in 5% non-fat milk, primary antibodies against FGF21 (ab171941, 1:1000), GPX4 (ab262509, 1:2000), SLC7A11 (ab307601, 1:1000), methyltransferase-like 14 (METTL14; ab220030, 1:1000), IGF2BP1 (ab184305, 1:1000) and glyceraldehyde-3-phosphate dehydrogenase (GAPDH) (ab181602, 1:5000; Abcam, Cambridge, UK) were used to incubate for 12 h with the membranes at 4°C. The membranes were then labeled with HRP-conjugated secondary antibodies (Abcam) for 2 h at 37°C. The bands were visualized using an ECL kit (Beyotime).

Cell counting kit-8 (CCK-8)

Following indicated treatment in a 96-well plate, PC12 cells (1×10^4 cells/well) were treated with 10 μ L CCK-8 solution for 2 h-incubation. Then the absorbance at 450 nm was detected using a microplate reader.

5-ethynyl-2'-deoxyuridine (EdU) assay

PC12 cells (2×10^5 cells/well) with indicated treatment were seeded onto 96-well plates and incubated for 2 h with 50 μ M EdU (Ribobio, Guangdong, China). Then cells were fixed with 4% paraformaldehyde, followed by dyeing with Apollp reaction cocktail. The DAPI was used to counterstain cell nucleus. Finally, EdU stained cells were captured and visualized.

Flow cytometry

After indicated treatment, PC12 cells were digested by 0.25% trypsin (Beyotime), centrifuged at $1000 \times g$ for 5 min and then washed with PBS. Then cells were harvested by centrifugation ($200 \times g$, 5 min) and re-suspended in 500 μ L Annexin-V binding buffer,

followed by staining with 10 μ L Annexin-V-FITC and 5 μ L propidium iodide (KeyGen, Nanjing, China) for 15 min in the dark. Apoptotic cells were detected by flow cytometer.

ELISA analysis

The supernatant of indicated PC12 cells were collected, then levels of IL-1 β and TNF- α were examined as per the instructions of ELISA kits (ELK Biotechnology, Wuhan, China).

Determination of iron ion

The intracellular levels of ferrous (Fe²⁺) ions were measured by using an iron assay kit (Abcam). PC12 cells with indicated treatment were lysed and centrifuged to obtain supernatant. Then cell supernatant was reacted with the assay buffer for 0.5 h, followed by incubating with iron probe for 1 h. Finally, the absorbance at 593 nm was read using a spectrophotometer to determine the Fe²⁺ concentration.

Reactive oxygen species (ROS) detection

PC12 cells with indicated treatment were stained with 10 mM DCFH-DA (Sigma-Aldrich) for 30 min at indoor temperature avoiding light. The fluorescence intensity was then detected to calculate intercellular ROS levels.

Measurement of glutathione (GSH)

The supernatant of PC12 cells with indicated treatment was obtained by centrifugation, then GSH levels were examined using a Reduced GSH assay kit (Nanjingjiancheng, Nanjing, China) following the recommended protocol.

Measurement of total N6-methyladenine (m6A)

Total RNA was isolated from PC12 cells with or without LPS exposure by TRIzol (Invitrogen), then the EpiQuik m6A RNA Methylation Quantification Kit (EpiGentek, NY, USA) was adopted to detect m6A levels.

Quantitative real-time PCR (qRT-PCR)

Total RNA was extracted from assigned PC12 cells by TRIzol (Invitrogen), then cDNAs were generated using the PrimeScript™ RT Reagent kit (Takara, Dalian, China), followed by qRT-PCR with the SYBR Green qPCR Master (Takara). Fold changes were assessed by the $2^{-\Delta\Delta C_t}$ method with GAPDH expression as the normalization. Table 1 shows qRT-PCR primers.

m⁶A RNA immunoprecipitation (MeRIP) assay

The isolated RNAs from assigned PC12 cells were fragmented into smaller fragments by ultrasound. Then 1 μ g fragments were suspended in immunoprecipitation buffer containing 3 μ g anti-m⁶A or anti-IgG or antibody, RNase inhibitor, protease inhibitor, and protein A magnetic beads, and incubated for 2 h at 4°C. After washing with proteinase, precipitated mRNAs were eluted and purified, and levels of FGF21 were detected by qRT-PCR.

Establishment of the SCI model

SD female rats (4-week-old, 220–250 g, n = 25) were purchased from Hunan Lake Jingda (Hunan, China) and adaptively fed for one week standardized conditions. Then rats were anaesthetized by inhaling 2–3% isoflurane. Then T9–11 spinous processes and lamina were exposed by stripping paravertebral muscles, and the spinous process and lamina of T10 were removed by a dorsal laminectomy. Next, a moderate contusion injury was induced using a 20 g impactor from a 3-cm height over 1 min. Rats in sham group underwent the same surgical procedure, but without compression. Contusion at the injured site, spasmodic swing of the tail and convulsions of both lower limbs are signs of successful modelling. Bladders were emptied 2–3 times a day until spontaneous urination to prevent urinary system infection. This animal study was performed based on the guidelines of the National Institutes of Health.

Rats were divided into five groups: Sham, SCI, SCI + Ad-sh-NC, SCI + Ad-sh-METTL14, and SCI + Ad-sh-METTL14 + Ad-sh-FGF21 groups. The recombinant adenovirus carrying METTL14 or FGF21 specific-short hairpin RNA (shRNA), or the scramble shRNA (sh-NC), named Ad-sh-NC, Ad-sh-METTL14 or Ad-sh-FGF21, were provided by HanBio (Shanghai, China). Rats in last three groups were injected with Ad-sh-NC, Ad-sh-METTL14 or Ad-sh-METTL14 + Ad-sh-FGF21 (1×10⁷/0.05 mL) via the tail vein once a day for 5

consecutive days. The Basso, Beattie & Bresnahan (BBB) scoring (ranging from 0 to 21 points) [4] was scored by two persons for three times at each time point of observation (1, 3, 5, 7 and 14 d) and then averaged to assess locomotor recovery. In addition, rats were euthanized with pentobarbital sodium (50 mg/kg) at day 28, spinal cord tissues were collected, fixed with 4% paraformaldehyde for one day, embedded in paraffin and cut into 3- μ m thickness for Nissl staining and haematoxylin and eosin (H&E) staining.

Statistical analysis

The data were expressed as mean \pm standard deviation (SD), and were analyzed by using Student's t-test or ANOVA followed by Tukeys post hoc test. $P < 0.05$ meant statistical significant.

RESULTS

FGF21 reverses LPS-induced proliferation inhibition, apoptosis and inflammation in neurons

As shown in Fig, 1A, we found that FGF21 expression was decreased by LPS treatment. Then we conduct gain-of-function assays. Western blotting analysis showed that FGF21 overexpression plasmids markedly elevated FGF21 expression in PC12 cells (Fig, 1B). After exposing to LPS, we found that FGF21 overexpression reversed LPS-induced viability inhibition (Fig, 1C) and reduction of EdU-positive cells (Fig, 1D), indicating the proliferation inhibition induced by FGF21 overexpression in LPS-treated OC12 cells. On the contrary, the LPS induced apoptosis in PC12 cells, which was also rescued by FGF21 overexpression (Fig, 1E). Moreover, FGF21 elevation reduced LPS-evoked increases of IL-1 β and TNF- α levels in PC12 cells (Fig, 1F).

FGF21 overexpression suppresses LPS-induced neuronal ferroptosis

As exhibited in Fig. 2A, CCK-8 analysis showed that ferrostatin-1, an inhibitor of ferroptosis could reverse LPS-induced viability inhibition in PC12 cells, suggesting that LPS-induced PC12 cell death may be related to ferroptosis. Then we investigated whether FGF21 was involved in LPS-induced ferroptosis. Ferroptosis is a new form of non-apoptotic cell

death marked by iron, oxidative modification, and GSH deficiency [28]. We observed that LPS treatment led to the increases of Fe²⁺ levels and ROS production, but caused the decrease of GSH levels in PC12 cells, while these changes were abolished by FGF21 overexpression (Fig. 2B–D), suggesting that FGF21 inhibited ferroptosis in PC12 cells under LPS treatment. In addition, we also found the protein levels of GPX4 and SLC7A11, two negative regulators of ferroptosis [19], were markedly reduced by LPS treatment in PC12 cells, while FGF21 overexpression could rescued LPS-induced decrease of their expression levels (Fig. 2E).

METTL14 induces FGF21 m6A modification in SCI cell models

We observed the m6A levels were increased in LPS-induced PC12 cells (Fig. 3A). Thereafter, SRAMP database predicted that FGF21 has m6A sites (Fig. 3B). MeRIP and qRT-PCR analyses showed that LPS treatment led to an increased m6A level in FGF21 (Fig. 3C), suggesting that LPS-induced PC12 cell injury might be associated with FGF21 m6A modification. Furthermore, we investigate which m6A methyltransferases mediates the methylation of FGF21, and found that only METTL14 knockdown negatively affected FGF21 expression in LPS-induced PC12 cells (Fig. 3D). Then western blotting analysis showed that LPS could elevate METTL14 levels in PC12 cells (Fig. 3E). After confirming the knockdown efficiency of si-METTL14 by western blotting (Fig. 3F), we discovered that METTL14 silencing decreased the m6A level of FGF21 in LPS-induced PC12 cells (Fig. 3G), demonstrating that METTL14 mediated the m6A methylation modification of FGF21 in SCI cell models.

IGF2BP1 is involved in regulating FGF21 expression by METTL14

Subsequently, we explored the m6A-binding proteins, including YTHDF1/2/3 and IGF2BP1/2/3, which might act on FGF21. Fig. 4A showed that only IGF2BP1 knockdown led to an increase of FGF21 expression in SCI cell models. RIP assay suggested that METTL14 knockdown decreased the enrichment of FGF21 on IGF2BP1 antibody (Fig. 4B). Then the IGF2BP1 overexpression plasmids were designed, and the transfection efficiency was

validated by western blotting in PC12 cells (Fig. 4C). Next, we demonstrated that IGF2BP1 overexpression caused the decrease of FGF21 expression in SCI cell models (Fig. 4D). Moreover, IGF2BP1 overexpression rescued METTL14 knockdown-induced elevation of FGF21 levels in LPS-induced PC12 cells (Fig. 4E). These data confirmed that METTL14 suppressed FGF21 expression in SCI cell models in m6A-IGF2BP1 dependent manner.

METTL14 silencing reverses LPS-induced neuronal apoptosis, inflammation and ferroptosis by regulating FGF21

To further study the role of METTL14 in LPS-induced neuronal injury by regulating FGF21, we constructed METTL14 and FGF21 knockdown cell models. Western blotting analysis showed that si-FGF21 introduction markedly reduced FGF21 expression in PC12 cells (Fig. 5A). Then the knockdown cell model was established in PC12 cells, followed by exposing to LPS. Functionally, we confirmed that METTL14 silencing rescued LPS-evoked inhibition of PC12 cell proliferation, while this effect was abolished by FGF21 silencing (Fig. 5B–D). The enhancement of apoptosis and the increases of IL-1 β and TNF- α caused by LPS in PC12 cells were impaired by METTL14 silencing, and then rescued in response to FGF21 silencing (Fig. 5E, F). Moreover, FGF21 silencing suppressed METTL14 deficiency-induced ferroptosis inhibition in LPS-treated PC12 cells, evidenced by increased Fe²⁺ levels (Fig. 5G), ROS production (Fig. 5H), decreased GSH contents (Fig. 5I) and reduced protein levels of GPX4 and SLC7A11 (Fig. 5J).

METTL14 silencing improves SCI and inhibits inflammation, apoptosis and ferroptosis in rat models by modulating FGF21 expression

SCI rat models were conducted in order to verify that METTL14 affects SCI progression by regulating FGF21 *in vivo*. Compared with the SCI + Ad-sh-NC group, mice in SCI + Ad-sh-METTL14 showed increased BBB locomotor scores, improved pathological conditions and decreased neuronal loss with increased NISSL body in spinal cord tissues, however, the protective effects mediated by Ad-sh-METTL14 were reversed by following FGF21 silencing (Fig. 6A, B). Moreover, we observed decreased levels of IL-1 β and TNF- α , and increased

protein levels of GPX4, SLC7A11 and FGF21 in SCI + Ad-sh-METTL14 group relative to SCI + Ad-sh-NC group, whereas further Ad-sh-FGF21 treatment averted the above-mentioned results (Fig. 6C–E).

DISCUSSION

In this study, we found that FGF21 levels were decreased in LPS-induced SCI cell models and SCI rat models. Functionally, we confirmed that FGF21 overexpression reversed LPS-induced proliferation inhibition, apoptosis and ferroptosis and promoted function recovery after SCI. Further mechanism analysis showed that the neuroprotective effects of FGF21 was negatively associated with METTL14 expression in SCI. Currently, several FGF21 mimetics and analogues have progressed to early phases of clinical trials in patients with non-alcoholic steatohepatitis, type 2 diabetes and obesity [10]. From a clinical perspective, FGF21 is a promising target to develop effective therapeutic strategies for ameliorating SCI.

METTL14 is one of important m6A methyltransferases forming the core heterodimer of the methyltransferase complex (MTC) that catalyzes methylation in RNA molecules [18]. m6A is the most prevalent posttranscriptional modification on eukaryotic mRNAs, and implicated in various aspects of biological processes ranging from cell differentiation, self-renewal, apoptosis and invasion by modulating mRNA expression [12, 13]. Importantly, abnormalities in m6A methylation after SCI have been identified, and m6A-related regulators participate in modulating nervous system development and function [17]. For example, METTL14 silencing promoted motor function and autophagy, and suppressed apoptosis in SCI rat models by increasing UBR1 levels via reducing UBR1 m6A modification [23]. METTL14 enhanced the apoptosis and inflammation in spinal cord neurons after SCI by inducing EEF1A2 m6A modification and reducing its expression [9]. The deficiency of METTL14 reduced the mature of pri-miR-375 by impairing its m6A modification, thereby attenuating SCI and suppressing neuronal apoptosis [24]. Herein, we also observed that METTL14 levels were increased in LPS-induced SCI cell models. Moreover, METTL14 induced FGF21 m6A modification, and reduced its expression. m6A reader proteins are

responsible for identifying m6A methylated transcripts and modulate almost all steps of mRNA metabolism, including RNA splicing, pre-mRNA processing, nuclear export, RNA degradation, stability and translation [6, 26]. We then validated that IGF2BP1 was involved in regulating FGF21 expression by METTL14, and METTL14 reduced FGF21 expression in an m6A-IGF2BP1 dependent mechanism. Functionally, METTL14 silencing reversed LPS-induced neuronal apoptosis, inflammation and ferroptosis, which were abolished by FGF21 silencing. In addition, METTL14 silencing improved SCI and repressed inflammation, apoptosis and ferroptosis in rat models by modulating FGF21 expression, further suggesting the potential application of FGF21 in SCI amelioration in an epigenetic dependent manner.

In conclusion, this study demonstrated that METTL14 knockdown attenuated neuronal inflammation, apoptosis and ferroptosis, and improved function recovery after SCI via up-regulating FGF21 in an m6A-IGF2BP1 dependent mechanism, highlighting the major pharmacological effects and potential application of FGF21 in SCI therapy.

ARTICLE INFORMATION AND DECLARATIONS

Data availability statement

The analyzed data sets generated during the study are available from the corresponding author on reasonable request.

Ethics statement

This animal study was performed based on the guidelines of the National Institutes of Health.

Authors' contributions

Guozhen Zhang conducted the experiments and drafted the manuscript. Bingbing Pu collected and analyzed the data. Fanjun Qin contributed the methodology, operated the software and edited the manuscript. Qiaojing Lin designed and supervised the study. All authors reviewed the manuscript.

Funding

None.

Acknowledgements

None.

Conflict of interest

The authors declare that they have no conflicts of interest.

REFERENCES

1. Adams AC, Yang C, Coskun T, et al. The breadth of FGF21's metabolic actions are governed by FGFR1 in adipose tissue. *Mol Metab.* 2012; 2(1): 31–37, doi: [10.1016/j.molmet.2012.08.007](https://doi.org/10.1016/j.molmet.2012.08.007), indexed in Pubmed: [24024127](https://pubmed.ncbi.nlm.nih.gov/24024127/).
2. Ahuja CS, Wilson JR, Nori S, et al. Traumatic spinal cord injury. *Nat Rev Dis Primers.* 2017; 3: 17018, doi: [10.1038/nrdp.2017.18](https://doi.org/10.1038/nrdp.2017.18), indexed in Pubmed: [28447605](https://pubmed.ncbi.nlm.nih.gov/28447605/).
3. Anjum A, Yazid MD, Fauzi Daud M, et al. Spinal cord injury: pathophysiology, multimolecular interactions, and underlying recovery mechanisms. *Int J Mol Sci.* 2020; 21(20), doi: [10.3390/ijms21207533](https://doi.org/10.3390/ijms21207533), indexed in Pubmed: [33066029](https://pubmed.ncbi.nlm.nih.gov/33066029/).
4. Basso DM, Beattie MS, Bresnahan JC. A sensitive and reliable locomotor rating scale for open field testing in rats. *J Neurotrauma.* 1995; 12(1): 1–21, doi: [10.1089/neu.1995.12.1](https://doi.org/10.1089/neu.1995.12.1), indexed in Pubmed: [7783230](https://pubmed.ncbi.nlm.nih.gov/7783230/).
5. Beattie MS, Hermann GE, Rogers RC, et al. Cell death in models of spinal cord injury. *Prog Brain Res.* 2002; 137: 37–47, doi: [10.1016/s0079-6123\(02\)37006-7](https://doi.org/10.1016/s0079-6123(02)37006-7), indexed in Pubmed: [12440358](https://pubmed.ncbi.nlm.nih.gov/12440358/).
6. Dou X, Huang L, Xiao Yu, et al. METTL14 is a chromatin regulator independent of its RNA N6-methyladenosine methyltransferase activity. *Protein Cell.* 2023; 14(9): 683–697, doi: [10.1093/procel/pwad009](https://doi.org/10.1093/procel/pwad009), indexed in Pubmed: [37030005](https://pubmed.ncbi.nlm.nih.gov/37030005/).
7. Eli I, Lerner DP, Ghogawala Z. Acute traumatic spinal cord injury. *Neurol Clin.* 2021; 39(2): 471–488, doi: [10.1016/j.ncl.2021.02.004](https://doi.org/10.1016/j.ncl.2021.02.004), indexed in Pubmed: [33896529](https://pubmed.ncbi.nlm.nih.gov/33896529/).
8. Flippo KH, Potthoff MJ. Metabolic messengers: FGF21. *Nat Metab.* 2021; 3(3): 309–317, doi: [10.1038/s42255-021-00354-2](https://doi.org/10.1038/s42255-021-00354-2), indexed in Pubmed: [33758421](https://pubmed.ncbi.nlm.nih.gov/33758421/).

9. Gao G, Duan Y, Chang F, et al. METTL14 promotes apoptosis of spinal cord neurons by inducing EEF1A2 m6A methylation in spinal cord injury. *Cell Death Discov.* 2022; 8(1): 15, doi: [10.1038/s41420-021-00808-2](https://doi.org/10.1038/s41420-021-00808-2), indexed in Pubmed: [35013140](https://pubmed.ncbi.nlm.nih.gov/35013140/).
10. Geng L, Lam KSL, Xu A. The therapeutic potential of FGF21 in metabolic diseases: from bench to clinic. *Nat Rev Endocrinol.* 2020; 16(11): 654–667, doi: [10.1038/s41574-020-0386-0](https://doi.org/10.1038/s41574-020-0386-0), indexed in Pubmed: [32764725](https://pubmed.ncbi.nlm.nih.gov/32764725/).
11. Gu Qi, Sha W, Huang Q, et al. Fibroblast growth factor 21 inhibits ferroptosis following spinal cord injury by regulating heme oxygenase-1. *Neural Regen Res.* 2024; 19(7): 1568–1574, doi: [10.4103/1673-5374.387979](https://doi.org/10.4103/1673-5374.387979), indexed in Pubmed: [38051901](https://pubmed.ncbi.nlm.nih.gov/38051901/).
12. Guan Q, Lin H, Miao L, et al. Functions, mechanisms, and therapeutic implications of METTL14 in human cancer. *J Hematol Oncol.* 2022; 15(1): 13, doi: [10.1186/s13045-022-01231-5](https://doi.org/10.1186/s13045-022-01231-5), indexed in Pubmed: [35115038](https://pubmed.ncbi.nlm.nih.gov/35115038/).
13. He L, Li H, Wu A, et al. Functions of N6-methyladenosine and its role in cancer. *Mol Cancer.* 2019; 18(1): 176, doi: [10.1186/s12943-019-1109-9](https://doi.org/10.1186/s12943-019-1109-9), indexed in Pubmed: [31801551](https://pubmed.ncbi.nlm.nih.gov/31801551/).
14. Jendelova P, Syková E, Jendelová P, et al. Bone marrow stem cells and polymer hydrogels — two strategies for spinal cord injury repair. *Cell Mol Neurobiol.* 2006; 26(7-8): 1113–1129, doi: [10.1007/s10571-006-9007-2](https://doi.org/10.1007/s10571-006-9007-2), indexed in Pubmed: [16633897](https://pubmed.ncbi.nlm.nih.gov/16633897/).
15. Li QS, Jia YJ. Ferroptosis: a critical player and potential therapeutic target in traumatic brain injury and spinal cord injury. *Neural Regen Res.* 2023; 18(3): 506–512, doi: [10.4103/1673-5374.350187](https://doi.org/10.4103/1673-5374.350187), indexed in Pubmed: [36018155](https://pubmed.ncbi.nlm.nih.gov/36018155/).
16. Lipinski MM, Wu J, Faden AI, et al. Function and mechanisms of autophagy in brain and spinal cord trauma. *Antioxid Redox Signal.* 2015; 23(6): 565–577, doi: [10.1089/ars.2015.6306](https://doi.org/10.1089/ars.2015.6306), indexed in Pubmed: [25808205](https://pubmed.ncbi.nlm.nih.gov/25808205/).
17. Liu D, Fan B, Li J, et al. N6-methyladenosine modification: a potential regulatory mechanism in spinal cord injury. *Front Cell Neurosci.* 2022; 16: 989637, doi: [10.3389/fncel.2022.989637](https://doi.org/10.3389/fncel.2022.989637), indexed in Pubmed: [36212687](https://pubmed.ncbi.nlm.nih.gov/36212687/).
18. Liu P, Li F, Lin J, et al. m6A-independent genome-wide METTL3 and METTL14 redistribution drives the senescence-associated secretory phenotype. *Nat Cell Biol.*

- 2021; 23(4): 355–365, doi: [10.1038/s41556-021-00656-3](https://doi.org/10.1038/s41556-021-00656-3), indexed in Pubmed: [33795874](https://pubmed.ncbi.nlm.nih.gov/33795874/).
19. Liu X, Chen C, Han D, et al. SLC7A11/GPX4 inactivation-mediated ferroptosis contributes to the pathogenesis of triptolide-induced cardiotoxicity. *Oxid Med Cell Longev.* 2022; 2022: 3192607, doi: [10.1155/2022/3192607](https://doi.org/10.1155/2022/3192607), indexed in Pubmed: [35757509](https://pubmed.ncbi.nlm.nih.gov/35757509/).
 20. Liu XH, Graham ZA, Harlow L, et al. Spinal cord injury reduces serum levels of fibroblast growth factor-21 and impairs its signaling pathways in liver and adipose tissue in mice. *Front Endocrinol (Lausanne).* 2021; 12: 668984, doi: [10.3389/fendo.2021.668984](https://doi.org/10.3389/fendo.2021.668984), indexed in Pubmed: [34046014](https://pubmed.ncbi.nlm.nih.gov/34046014/).
 21. Nogueira-Rodrigues J, Leite SC, Pinto-Costa R, et al. Rewired glycosylation activity promotes scarless regeneration and functional recovery in spiny mice after complete spinal cord transection. *Dev Cell.* 2022; 57(4): 440–450.e7, doi: [10.1016/j.devcel.2021.12.008](https://doi.org/10.1016/j.devcel.2021.12.008), indexed in Pubmed: [34986324](https://pubmed.ncbi.nlm.nih.gov/34986324/).
 22. Shinozaki M, Nagoshi N, Nakamura M, et al. Mechanisms of stem cell therapy in spinal cord injuries. *Cells.* 2021; 10(10): 2676, doi: [10.3390/cells10102676](https://doi.org/10.3390/cells10102676), indexed in Pubmed: [34685655](https://pubmed.ncbi.nlm.nih.gov/34685655/).
 23. Wang C, Zhu X, Chen R, et al. Upregulation of UBR1 m6A methylation by METTL14 inhibits autophagy in spinal cord injury. *eNeuro.* 2023; 10(6), doi: [10.1523/ENEURO.0338-22.2023](https://doi.org/10.1523/ENEURO.0338-22.2023), indexed in Pubmed: [37094938](https://pubmed.ncbi.nlm.nih.gov/37094938/).
 24. Wang H, Yuan J, Dang X, et al. Mettl14-mediated m6A modification modulates neuron apoptosis during the repair of spinal cord injury by regulating the transformation from pri-mir-375 to miR-375. *Cell Biosci.* 2021; 11(1): 52, doi: [10.1186/s13578-020-00526-9](https://doi.org/10.1186/s13578-020-00526-9), indexed in Pubmed: [33706799](https://pubmed.ncbi.nlm.nih.gov/33706799/).
 25. Werner C, Engelhard K. Pathophysiology of traumatic brain injury. *Br J Anaesth.* 2007; 99(1): 4–9, doi: [10.1093/bja/aem131](https://doi.org/10.1093/bja/aem131), indexed in Pubmed: [17573392](https://pubmed.ncbi.nlm.nih.gov/17573392/).
 26. Adhikari S, Xiao W, Zhao YL, et al. Nuclear m(6)A reader YTHDC1 regulates mRNA splicing. *Mol Cell.* 2016; 61(4): 507–519, doi: [10.1016/j.molcel.2016.01.012](https://doi.org/10.1016/j.molcel.2016.01.012), indexed in Pubmed: [26876937](https://pubmed.ncbi.nlm.nih.gov/26876937/).

27. Xu T, Zhu Q, Huang Q, et al. FGF21 prevents neuronal cell ferroptosis after spinal cord injury by activating the FGFR1/ β -Klotho pathway. *Brain Res Bull.* 2023; 202: 110753, doi: [10.1016/j.brainresbull.2023.110753](https://doi.org/10.1016/j.brainresbull.2023.110753), indexed in Pubmed: [37660729](https://pubmed.ncbi.nlm.nih.gov/37660729/).
28. Yu Yi, Yan Y, Niu F, et al. Ferroptosis: a cell death connecting oxidative stress, inflammation and cardiovascular diseases. *Cell Death Discov.* 2021; 7(1): 193, doi: [10.1038/s41420-021-00579-w](https://doi.org/10.1038/s41420-021-00579-w), indexed in Pubmed: [34312370](https://pubmed.ncbi.nlm.nih.gov/34312370/).
29. Zhu S, Ying Y, Ye L, et al. Systemic administration of fibroblast growth factor 21 improves the recovery of spinal cord injury (SCI) in rats and attenuates SCI-induced autophagy. *Front Pharmacol.* 2020; 11: 628369, doi: [10.3389/fphar.2020.628369](https://doi.org/10.3389/fphar.2020.628369), indexed in Pubmed: [33584310](https://pubmed.ncbi.nlm.nih.gov/33584310/).

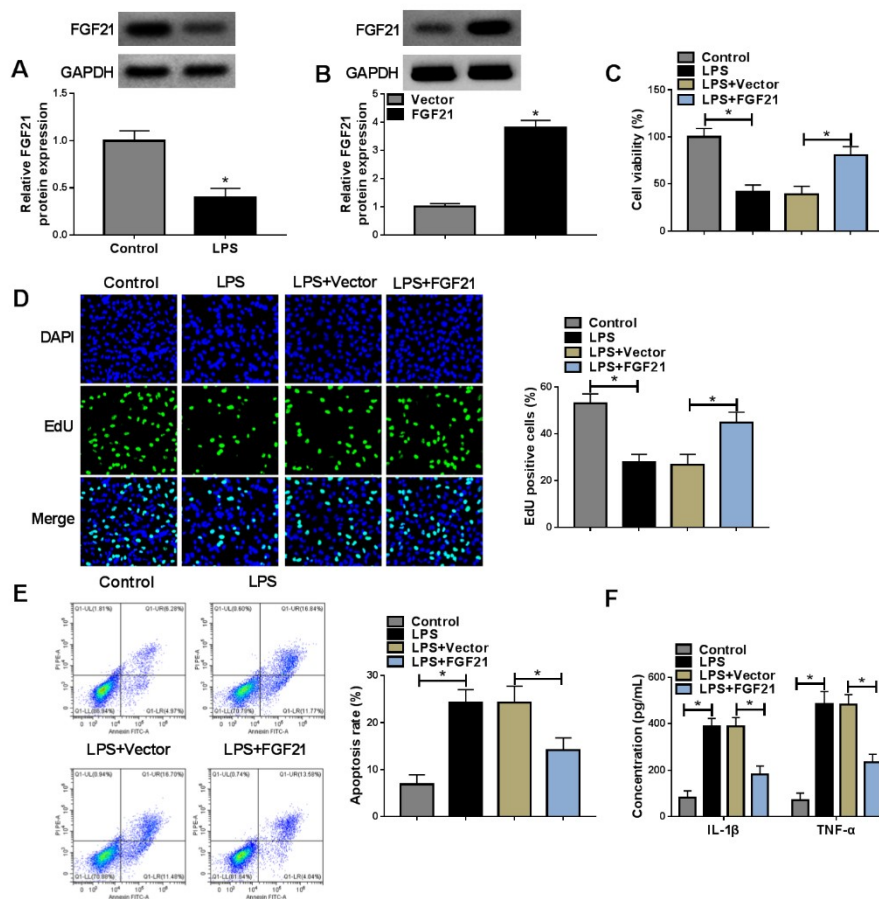


Figure 1. FGF21 overexpression reverses LPS-induced neuronal apoptosis and inflammation; **A.** Western blotting analysis for FGF21 expression in PC12 cells treated with or without LPS

(the grouping of bots were cropped from different gels); **B**. The transfection efficiency of FGF21 was validated using western blotting in PC12 cells; **C–F**. PC12 cells were transfected with FGF21 or Vector, followed by LPS treatment; **C**, **D**. CCK-8 and EdU assays for cell proliferation; **E**. Flow cytometry for cell apoptosis; **F**. ELISA analysis for IL-1 β and TNF- α levels in cells. *P < 0.05. CCK-8 — cell counting kit-8; EdU — 5-ethynyl-2'-deoxyuridine assay; FGF21 — fibroblast growth factor 21; GAPDH — glyceraldehyde-3-phosphate dehydrogenase; LPS — lipopolysaccharide.

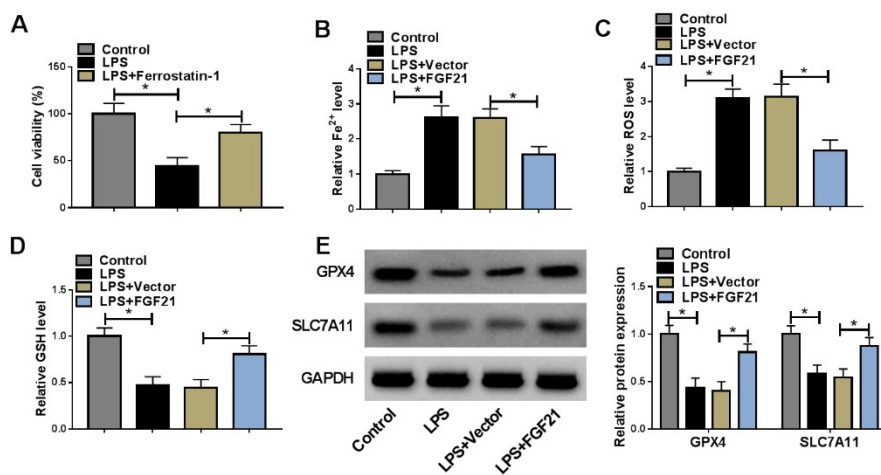


Figure 2. FGF21 overexpression reverses LPS-induced neuronal ferroptosis; **A**. CCK-8 assay for the viability of LPS-induced PC12 cells that were pre-treated with Ferrostatin-1; **B–E**. PC12 cells were transfected with FGF21 or Vector, followed by LPS treatment; **B**. Fe²⁺ detection by the kit; **C**. Detection of ROS levels by DCFH-DA probe; **D**. GSH detection by the kit; **E**. Western blotting analysis for protein levels of GPX4 and SLC7A11 (the grouping of bots were cropped from different gels). *P < 0.05. CCK-8 — cell counting kit-8; FGF21 — fibroblast growth factor 21; GAPDH — glyceraldehyde-3-phosphate dehydrogenase; GSH — glutathione; LPS — lipopolysaccharide.

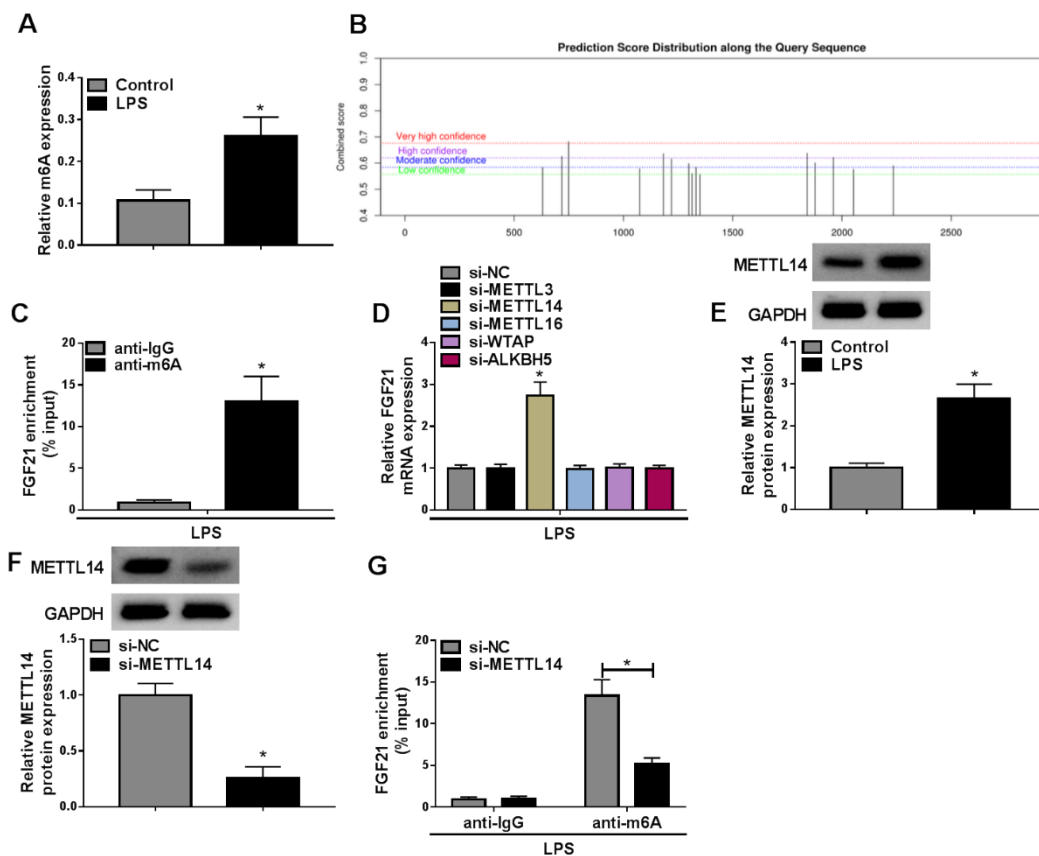


Figure 3. METTL14 induces FGF21 m6A modification in SCI cell models; **A.** Detection of m6A levels in LPS-induced PC12 cells; **B.** SRAMP database predicts that FGF21 has m6A sites; **C.** MeRIP and qRT-PCR analyses investigated the FGF21 m6A modification level in PC12 cells; **D.** The effects of methyltransferases knockdown on the expression change of FGF21 in LPS-induced PC12 cells were analyzed by qRT-PCR; **E.** Western blotting analysis for METTL14 expression in PC12 cells treated with or without LPS (the grouping of bots were cropped from different gels); **F.** The knockdown efficiency of si-METTL14 and si-NC was validated using western blotting (the grouping of bots were cropped from different gels); **G.** MeRIP and qRT-PCR analyses investigated the FGF21 m6A modification level in PC12 cells after si-METTL14 or si-NC transfection. * $P < 0.05$. FGF21 — fibroblast growth factor 21; GAPDH — glyceraldehyde-3-phosphate dehydrogenase; LPS — lipopolysaccharide; SRAMP — SNP-related amino acid mutation prediction.

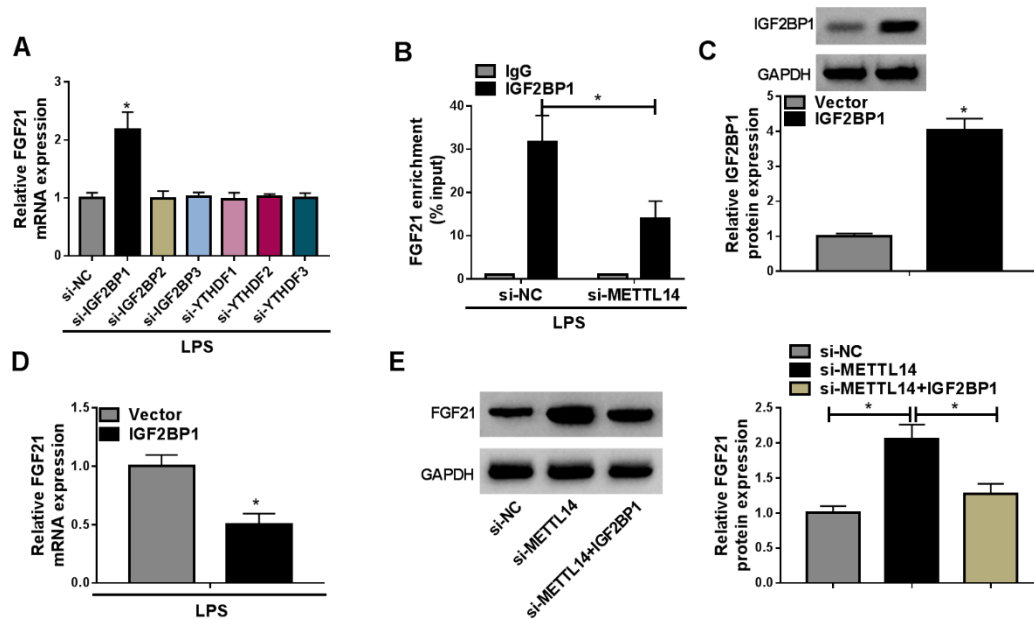


Figure 4. IGF2BP1 is involved in regulating FGF21 expression by METTL14; **A.** The effects of the knockdown of m6A “readers” on the expression change of FGF21 in LPS-induced PC12 cells were analyzed by qRT-PCR; **B.** RIP assay was used to investigate the binding between FGF21 and IGF2BP1 in LPS-treated PC12 cells with si-METTL14 or si-NC transfection; **C.** The transfection efficiency of IGF2BP1 or Vector was validated using western blotting in PC12 cells; **D.** Western blotting analysis for FGF21 expression in LPS-induced PC12 cells that were transfected with IGF2BP1 or Vector (the grouping of bots were cropped from different gels); **E.** Western blotting analysis for FGF21 expression in PC12 cells transfected with si-METTL14 alone or si-METTL14 and IGF2BP1. * $P < 0.05$. FGF21 — fibroblast growth factor 21; LPS — lipopolysaccharide; METTL14 — methyltransferase-like 14; qRT-PCR — quantitative reverse transcription polymerase chain reaction; RIP assay — RNA immunoprecipitation assay; si-NC — small interfering RNA negative control.

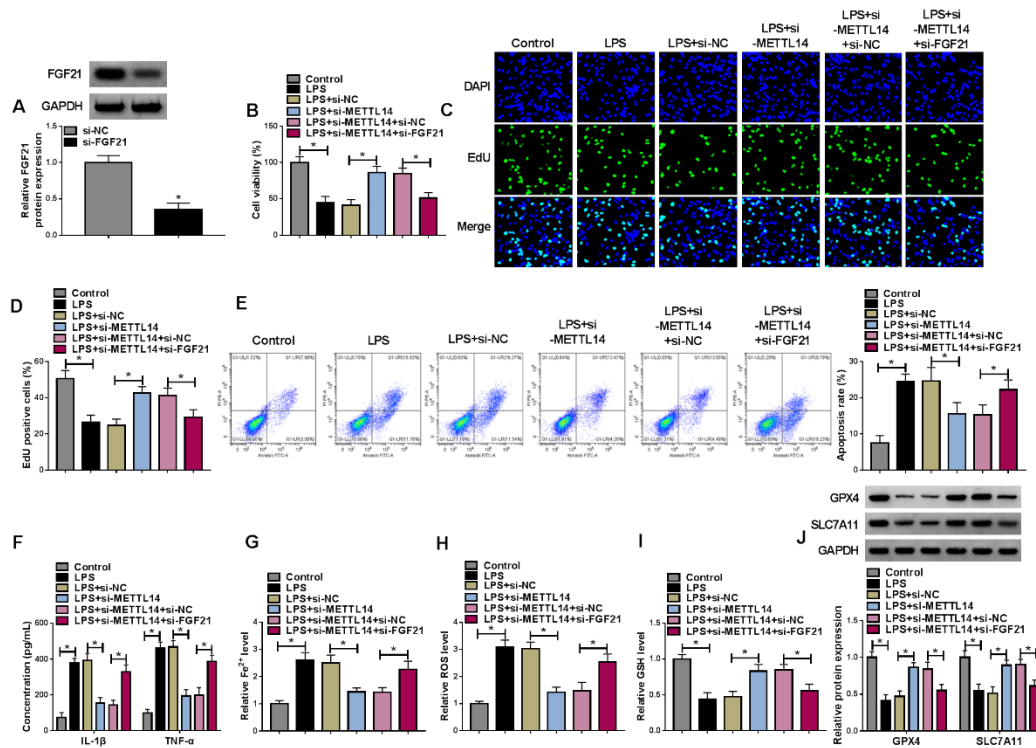


Figure 5. METTL14 silencing reverses LPS-induced neuronal apoptosis, inflammation and ferroptosis by regulating FGF21; **A**. The knockdown efficiency of si-NC or si-FGF21 was verified using western blotting in PC12 cells (the grouping of bots were cropped from different gels); **B–J**. PC12 cells were transfected with si-METTL14 alone or si-METTL14 and si-FGF21, followed by LPS treatment; **B–D**. CCK-8 and EdU assays for cell proliferation; **E**. Flow cytometry for cell apoptosis; **F**. ELISA analysis for IL-1 β and TNF- α levels in cells; **G**. Fe²⁺ detection by the kit; **H**. Detection of ROS levels by DCFH-DA probe; **I**. GSH detection by the kit; **J**. Western blotting analysis for protein levels of GPX4 and SLC7A11 (the grouping of bots were cropped from different gels). *P < 0.05. CCK-8 — cell counting kit-8; EdU — 5-ethynyl-2'-deoxyuridine assay; FGF21 — fibroblast growth factor 21; GSH — glutathione; LPS — lipopolysaccharide; METTL14 — methyltransferase-like 14; si-NC — small interfering RNA negative control.

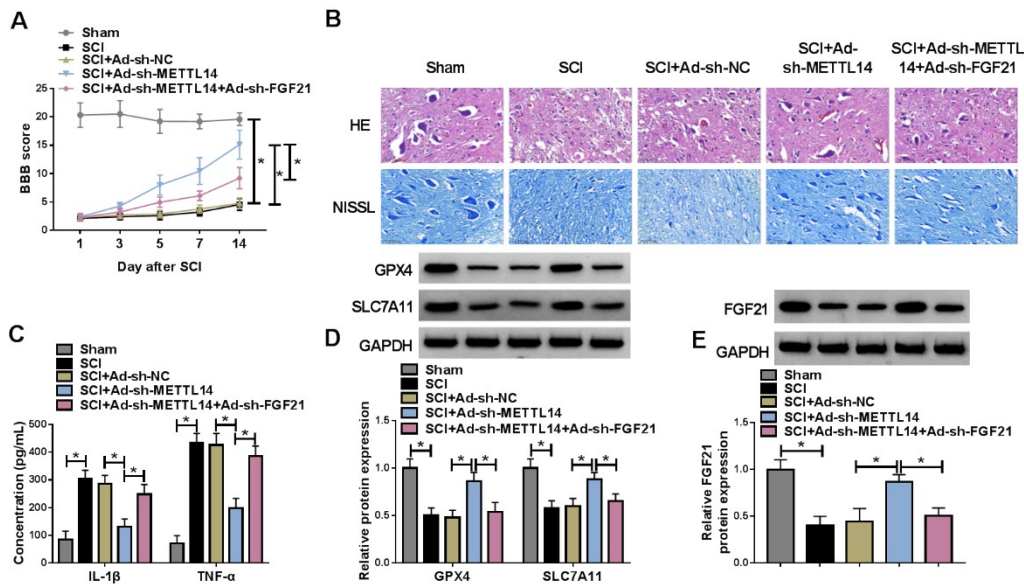


Figure 6. METTL14 silencing improves SCI and inhibits inflammation, apoptosis and ferroptosis in rat models by modulating FGF21 expression; **A.** Locomotor ability detected by Basso, Beattie and Bresnahan (BBB) locomotor rating scale; **B.** H&E and Nissl-staining for pathological conditions of spinal cord tissues; **C.** ELISA analysis for IL-1 β and TNF- α levels; **D, E.** Western blotting analysis for protein levels of GPX4, SLC7A11 and FGF21 (the grouping of bots were cropped from different gels). *P < 0.05. FGF21 — fibroblast growth factor 21; H&E — haematoxylin and eosin; SCI — spinal cord injury

Table 1. The primer for qRT-PCR.

Name	Primers for qRT-PCR (5'-3')	
FGF21	Forwar	GTCTGAACCTGACCCATCCC
	d	
METTL14	Reverse	ATCCATTCCATCAGGGCTGC
	Forwar	TGGAAATAGGTGCGCAGAGG
IGF2BP1	d	
	Reverse	GTTCTACTCGGGTTCCCAGC
GAPDH	Forwar	GCCCTGGATCTCGTCTTTGAA
	d	
GAPDH	Reverse	CCATTCTCAGGACCTTGCGT
	Forwar	GGTGAAGGTCGGTGTGAACG
GAPDH	d	
	Reverse	CTCGCTCCTGGAAGATGGTG

FGF21 — fibroblast growth factor 21; GAPDH — glyceraldehyde-3-phosphate dehydrogenase; IGF2BP1 — insulin-like growth factor 2 mRNA-binding protein 1; METTL14 — methyltransferase-like 14.